109011

TRAC PERFORMANCE ESTIMATES

A Final Report
For Grant
NAG 9-362

Submitted to:
L. Monford
and
R. Berka
NASA JSC
Mail Code ER4
Houston, Texas 77058

by:
L. Everett
Mechanical Engineering Department
Texas A&M University
College Station, Texas 77843-3123

July 22, 1992

TRAC PERFORMANCE ESTIMATES

A Final Report

For Grant

NAG 9-362

Submitted to:

L. Monford

and

R. Berka

NASA JSC

Mail Code ER4

Houston, Texas 77058

by:

L. Everett

Mechanical Engineering Department

Texas A&M University

College Station, Texas 77843-3123

July 22, 1992

ABSTRACT

This report documents the performance characteristics of a TRAC (Targeting Reflective Alignment Concept) sensor. The performance will be documented for both short and long ranges. For long ranges, the sensor is used without the flat mirror attached to the target.

To better understand the capabilities of TRAC based sensors, an engineering model is required. The model can be used to better design the system for a particular application. This is necessary because there are many interrelated design variables in the TRAC system. These include lense parameters, camera, and target configuration.

The report presents first an analytical development of the performance, and second an experimental verification of the equations. In the analytical presentation it is assumed that the best vision resolution is a single pixel element. The experimental results suggest however that the resolution is better than 1 pixel. Hence the analytical results should be considered worst case conditions.

The report also discusses advantages and limitations of the TRAC sensor in light of the performance estimates. Finally the report discusses potential improvements.

SCOPE AND OBJECTIVES

This report documents a small portion of the TRAC related projects performed by the PI's and is the first in a series of reports. Copies of all reports will be forwarded to L. Monford, and R. Berka, both of NASA JSC.

The TRAC targeting system was automated using image processing hardware, a PC and a PUMA. The automation system, software and hardware, will be documented in a report submitted in the near future and in a master's thesis by Mike Bradham.

The automated TRAC (because of the relatively slow video rates) could not be used for servo control of the robot. Therefore on velocity driven robots (as in our case and the MDF) it was necessary to design a position control. Several control methods were used and tested. These algorithms will be discussed in a master's thesis by Jeff Pafford.

The automated TRAC was implemented on the MDF during the summer of 1991. One problem confronted during the implementation was to determine the robot's dynamic response. An estimate of the robot's response was determined from input/output data and will be documented in a master's thesis by Ravishankar Sreekantappa.

In addition to these theses and reports, several papers have been and will continue to be submitted for publication. When these papers are accepted for publication, copies will be forwarded to NASA.

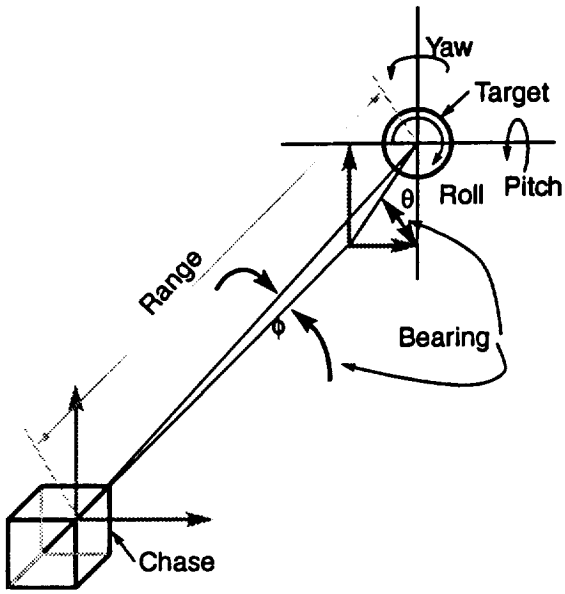

Figure 1: Definition of Errors.

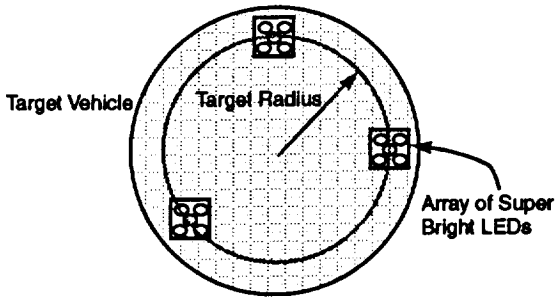

Figure 2: Active Beacon Target for Long Range Operations.

TRAC SENSOR OPERATION

The sensing system studied and reported on is an autonomous version of the Tracking and Reflective Alignment Sensor (TRAC) [1]. Figure 1 shows the definitions of the target bearing, range, roll, pitch (yaw is similar). Not shown in the figure are transverse deviations. These deviations are the two translations perpendicular to the range.

The TRAC sensing concept has two distinct operating modes, one for short range operations and the other for longer ranges. This report will discuss the performance of both modes.

Long Range Operations

At large ranges, range and bearing sensing is most critical. Figure 2 shows a target

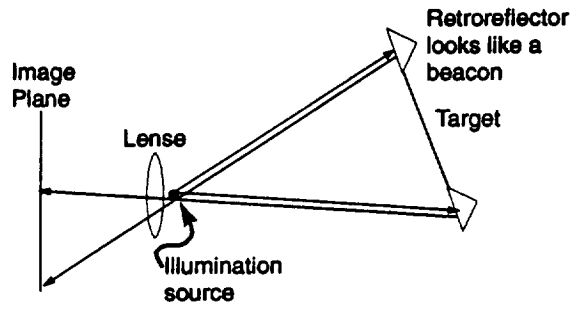

Figure 3: Using Retroreflectors with TRAC to Produce Beacons.

with three arrays of very bright LEDs mounted at a target radius. These beacons are flashed on and off at approximately the frame rate. The centroid of these beacons in the image allow the bearing angles (or alternatively the transverse displacement) to be computed. The perimeter formed by the beacons determine the range. The orientation of the target is determined by a perspective transformation using the three beacons. The ambiguity arising from using three rather than four points in the transformation is not resolved with just the three bright targets.

In long range applications, the TRAC system determines an object pose as any conventional vision based sensor.

Short Range Operations

When the target is at a small range[1] the targeting concept can implement a conventional TRAC algorithm. The TRAC algorithm uses a flat mirror and three retroreflectors mounted on a target. For our work the retroreflectors are mounted in a triangular pattern where one leg is significantly shorter than the other two.

Lighting for the TRAC sensor (the camera) is mounted on the camera itself. In some applications, the illumination is in the dead center of the lense, on others it is on the edge of the lense. The light illuminates the flat mirror and the reflectors.

The reflector image is used with an algorithm similar to that used with the beacons to determine range, bearing, and roll. Figure 3 shows how this is accomplished. Because the retro reflectors bounce light back in the direction it came from, their location on the image plane is independent of the orientation of the target. At least to the extent that target rotation does not affect the position of the retros. Of course if the retros were on the tip of a post, their position would be more of a function of target orientation.

The image produced by the flat mirror is used to determine yaw and pitch. Figure 4 shows how this is done. The software algorithm will not be explained here, the interested reader should consult [2].

[1] Exactly what small means depends on the capture angle of the TRAC mirror, the uncertainty in the target location and the maneuverability of the chase vehicle (or robot).

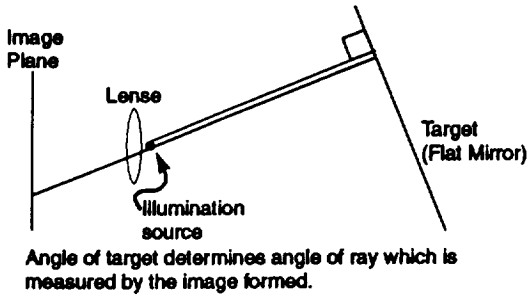

Figure 4: Using Retroreflectors with TRAC to Produce Beacons.

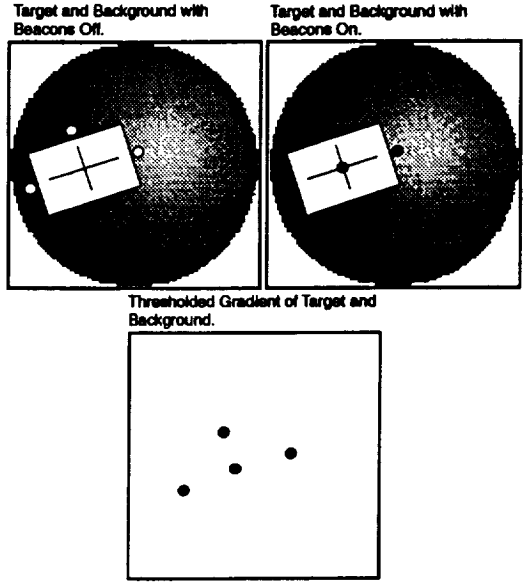

Figure 5: The Essence of the Filtering Technique Used.

Vision Robustness

One very serious problem with any autonomous sensing system is robustness to extraneous sensations. In the case of a vision system, we need to be robust to background lighting, changes in illumination, occlusion and the like. We chose to use structured lighting as the solution to robustness.

Noise rejection is obtained by time domain sampling the image thus blacking all pixels which do not blink at the known rate of our source lights. Essentially, this is a filtering (or sampling) method. To reduce computational overhead, the lights are blinked to enable a simple filter arrangement to operate. Figure 5 shows a TRAC target illuminated by a source on the camera. The image contains a background, a flat mirror and three retroreflectors. Two images (for example) are taken in sequence and subtracted to determine the gradient of intensity for each pixel. Only the pixels that change produce bright spots in the image.

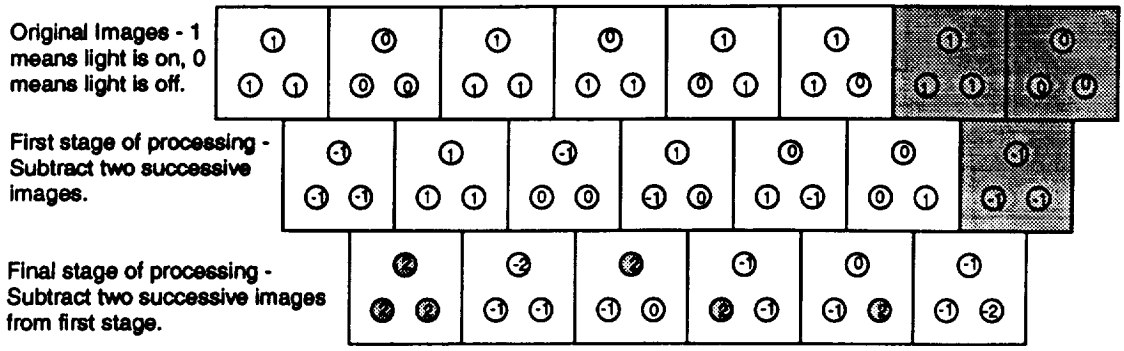

Figure 6: "Filter" Algorithm for Reducing Background Light Effects.

Of course, motion also produces a gradient and therefore one would expect some of the background to make it into the image. To reduce this effect, the second derivative (change of the gradient) could be computed. Figure 6 shows how the algorithm could be implemented for beacons, a similar procedure could be used for the short range TRAC. Once the camera synchronizes with the beacons, we have images as shown in the first row. For simplicity the figure does not show background. If we have control over the beacons, obtaining the images in the top row is possible. Next we subtract successive images to obtain images in the second row. Since this is simply a gradient, there will of course be some background due to, for example, motion. At this stage, pixel amplitude can be positive, negative or zero. Most of the background will be close to zero. Images in the third row are determined by subtracting consecutive images in the second row. Essentially this is the second differential of the pixels. As you can see in the third row images, certain beacons have become accentuated because they were illuminated then dimmed at specific times. Now it is true that some background could become accentuated as well, provided it increases and decreases its brilliance at the correct time, however the probability of that is expected to be small. After the second differential has been taken, the pixels will be thresholded at a level determined by the maximum brilliance. What is expected in the image is either all, none or one beacon (we will know which).

The intensity of background lighting could be reduced further by using an interference optical filter which passes only the light color emitted by our relatively single color, blinking illumination source. In our applications we never had the need for these filters.

NOMENCLATURE

This section introduces some basic nomenclature used throughout the report.

1. Nearest Distance in Focus - d_n - A lense will have a range of distances to objects which are in sharp focus. This is the minimum of these distances. It is measured from the center of the lense.

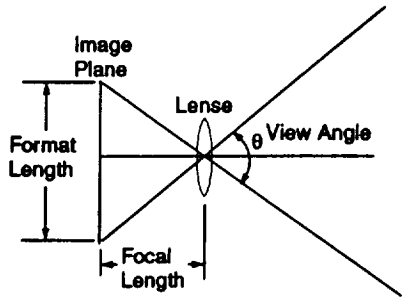

Figure 7: Definition of the View Angle.

2. Farthest Distance in Focus - d_f - See Nearest Distance in Focus. This is the maximum distance in focus.

3. Distance Focused On - d_{focus} - Depending on the location of the image plane, there is a range (measured from the lense center) at which the focus is perfect.

4. View Angle - Θ - This is twice the maximum angle measured from the optical axis at which light rays will hit the image plane. Figure 7 shows its definition.

5. View Angle at Focus - θ - This is twice the maximum angle measured from the optical axis at which light rays will hit the image plane. It differs from Θ in that the image plane is at the focus distance.

6. Focal Length - f - One of the two independent variables in a lense. The distance measured from the lense center at which parallel light rays intersect at a point. It is the distance to place the image plane to focus on an object at infinity.

7. Distance to Image Plane - f_i - The distance measured from the lense center to the location of the image plane.

8. F Stop - F_s - One of the two independent variables in a lense. It is a dimensionless ratio of the focal length over the lense diameter. It is a unitless way of describing how much light can enter the lense. The smaller the number the more light can enter. In a sense, all lenses with a given F Stop allow the same amount of light intensity to enter.

9. Pixel Size - x_∞ - The real size of an object when the image plane is at the focal length.

10. Pixel Size at Focus - x_f - The real size of a focused object which exactly covers one pixel.

11. Format Edge Length - l_f - The length along one edge of the image plane.

12. Circle of Confusion - l_c - When light from a single source enters the lense, it is bent into a cone like arrangement. If the image is not perfectly focused on the image plane, the light rays form a circular like shape. The largest diameter circle which still looks like a single point is the circle of confusion.

13. Range to Object - d - The distance measured from the lense center to an object.

14. Number of Pixel Rows - n_p - The number of rows of pixels in the image plane.

15. Pixel - p - A distance measured in the image plane. It is a discrete number with units of "pixels".

16. Diameter of Target - D_t - The diameter of a target.

17. Sampling Period - τ - The time between samples of images.

18. Bearing - γ - The angle between a line drawn from the lense center to an object and the optical axis.

19. Perimeter - D_p - The perimeter of the target.

20. Transverse Position - y - A distance perpendicular to the optical axis.

VIDEO EQUIPMENT

This section presents a summary of the basic equations for choosing lenses, camera resolutions and the like. All of these equations are straightforward and can be found in most texts on photography. They are included only to assist those inexperienced in the area.

Lenses

There are two free parameters in a simple lense, the diameter and the focal length. The focal length (f) is the distance from the center of the lense to the point of focus of an object located infinitely in front of the lense. The Fstop (F_s) is a dimensionless ratio of the focal length over the lense diameter. Once these parameters are specified, the lense is unique. In our calculations however there are several other quantities which make the calculations simpler.

Basic Vision System Specifications. There are a set of basic specifications for the vision system which can be used more effectively to choose a lense. Somewhat arbitrary (but realistic) values of these parameters are shown in Table 1^2. These numbers are used in the performance equations whenever a numerical example is

Parameter	Value
Smallest Range to Focus on	5.4 feet
Greatest Range to Focus on	13.5 feet
Desired Fstop Value	3.8
Diagonal Format Length	0.5 inch
Number of Pixel Rows	512
Circle of Confusion	1 Pixel
Focal Length (Experimental Hardware)	19 mm
Radius of Beacon Target	1 foot
Radius of Reflector Target	20 mm
TRAC Mirror Edge Length	1 foot

Table 1: Basic Vision System Parameters.

given. In actuality, all calculations were relatively insensitive to the greatest range parameter for distances greater than 100 feet. The desired Fstop value for orbit operations was estimated to be about 22 (after experimenting with a camera and target system in bright daylight), however 3.8 is used in the calculations because it matches our experimental equipment. The format length was chosen based on the fact that a typical half inch format has a good signal to noise ratio [3] (it just happens to match our hardware). The number of pixels matches our hardware.

Notice that we are specifying three quantities to define the lense system. These are: the Fstop, the closest focused distance and the greatest focused distance. To satisfy these three specifications with our lense, we must select the focal length, Fstop and the point of focus (eg. where to place the image plane). To do this, we establish a relation between the specifications and the distance to a sharply focused object. Figure 8 helps with the derivation. The point of focus in each case shown is found by determining the intersection of the lines on the image plane. The intersection point f_i can be expressed in terms of the range d_{focus} as:

$$f_i = \frac{1}{\frac{1}{f} - \frac{1}{d_{\text{focus}}}}$$

As shown in part (d) of Figure 8, the near and far focus ranges can be determined by equating the separation distance (measured on the image plane) between light rays

[2]Actually the smallest and greatest range to focus on along with the Fstop are more convenient to specify when you are selecting from a large assortment of lenses therefore the analysis is written in terms of these values. From these, the focal length and position of the image plane can be computed as is done in the analysis. However, during the experimental investigations, we were forced to use a lense which was available, therefore the focal length was fixed. The values shown in Table 1 were selected to match our experimental lense

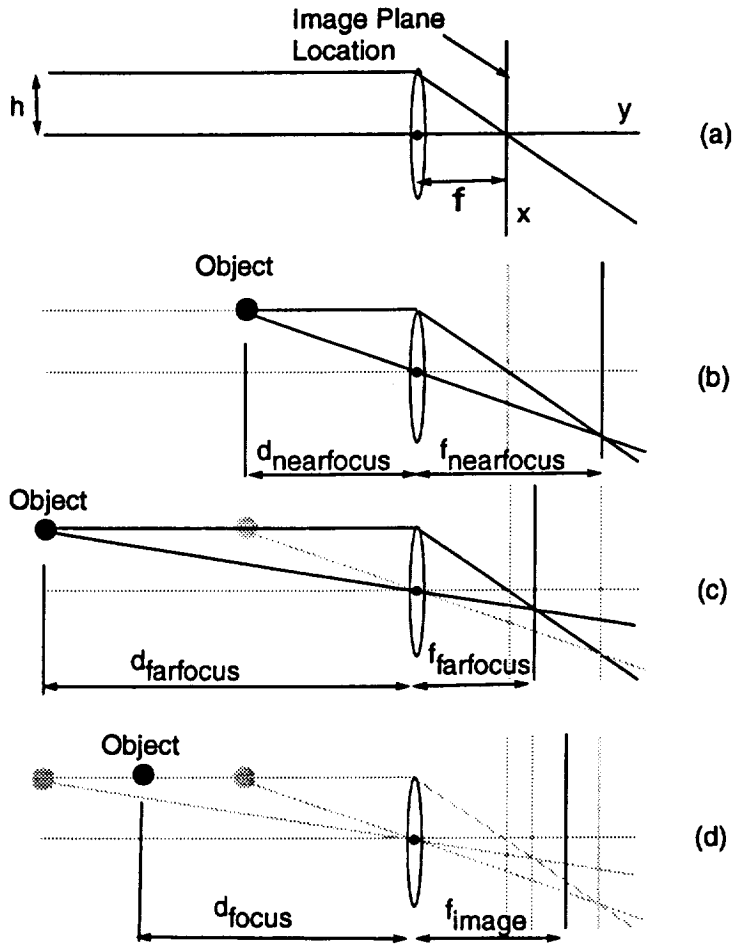

Figure 8: A Simple Lens Focused On (a) An Object At Infinity, (b) An Object Close In, (c) An Object Far Away, and (d) An Object At An Arbitrary Distance.

originating from the object the circle of confusion. For an object at d range and an image plane at f_i the separation distance (s) is (using the definition of Fstop):

$$s = \frac{-(d\,f) + d\,f_i - f\,f_i}{2\,d\,F_s}$$

Equating $\pm 2s$ to the circle of confusion, we solve for d which is the near and far ranges in focus. These are:

$$d_n = \frac{-1.\,f\,f_i}{f - 1.\,f_i - 1.\,l_c\,F_s} \tag{1}$$

and:

$$d_f = \frac{f\,f_i}{-1.\,f + f_i - 1.\,l_c\,F_s} \tag{2}$$

Now equations 1 and 2 are convenient if one has a given lens (F_s and f are given) however for the selection of the lens it is better to invert these to solve for f and f_i. These inversions provide the following:

$$f = \frac{l_c\,F_s - \frac{2\,l_c\,d_f\,F_s}{d_f - d_n} + \frac{\sqrt{l_c}\,\sqrt{F_s}\,\sqrt{l_c\,{d_f}^2\,F_s + 8\,{d_f}^2\,d_n + 2\,l_c\,d_f\,F_s\,d_n - 8\,d_f\,{d_n}^2 + l_c\,F_s\,{d_n}^2}}{d_f - d_n}}{2}$$

and:

$$f_i = \frac{\frac{l_c\,F_s\,(d_f + d_n)}{d_f - d_n} + \frac{\sqrt{l_c}\,\sqrt{F_s}\,\sqrt{l_c\,{d_f}^2\,F_s + 8\,{d_f}^2\,d_n + 2\,l_c\,d_f\,F_s\,d_n - 8\,d_f\,{d_n}^2 + l_c\,F_s\,{d_n}^2}}{-d_f + d_n}}{2} \tag{3}$$

As expected, the focal length increases with the average distance in focus and decreases with the depth of field.

View Angles

The view angle can be computed based on the focal length and the format length. Figure 7 shows the definition of the view angle. The angle shown is the angle when the lense is focused at infinity. It is computed as:

$$\Theta = 2\tan^{-1}\left(\frac{l_f}{2f}\right) = 2\,\tan^{-1}\left(\frac{l_f}{2\,f}\right)$$

The view angle at focus θ can be computed similarly when the distance to the image plane is known as:

$$\theta = 2\,\tan^{-1}\left(\frac{l_f}{2\,f_i}\right)$$

Location of Focused Object

When focused at infinity, the image plane will be located at the focal length. When the lense is focused at some other point (the point of focus) the image plane will be located at f_i given in equation 3.

POSE CALCULATIONS AND RESOLUTION

Rate Determination

The rate of change of a signal is determined by differencing successive values. For example, if S_i is the signal at sample period i, then the derivative is approximately:

$$\dot{S}_i \approx \frac{S_i - S_{i-1}}{\delta}$$

Hence the error in the derivative calculation (due to measurement error) is a function of the signal error and the time error. We assume we have a very precise time measurement, therefore our derivative signal error is:

$$\Delta\dot{S} \approx \frac{2\Delta S}{\delta}$$

With the sampling time set to 0.1 seconds (three frames), the velocity error is 20 times the signal error.

Pixel Sizes

When determining the position of a feature on the image plane, the camera measures position in pixels. A simple relationship can be determined which gives the actual size of a pixel. This relationship depends on where the image plane is and the range to the object. The pixel size when the image plane is at the point of focus is:

$$x_f = \frac{d\, l_f}{f_i\, n_p}$$

One pixel is what we assume is the smallest change in target position which can be measured. This of course assumes we cannot perform subpixel accuracy calculations. Figure 9 shows the relationship between the pixel size and range for the specifications given earlier. Figure 10 shows the relationship of pixel size to the Fstop. Figure 11 shows the relationship between the focus distance (indirectly the image plane position) and pixel size is immaterial at distances above 50 meters.

The term pixel size means the actual height of an object which fills up one pixel height on the image plane.

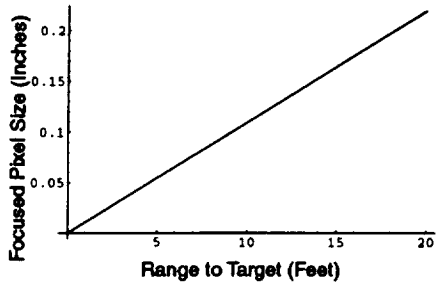

Figure 9: Focused Pixel Size versus Range.

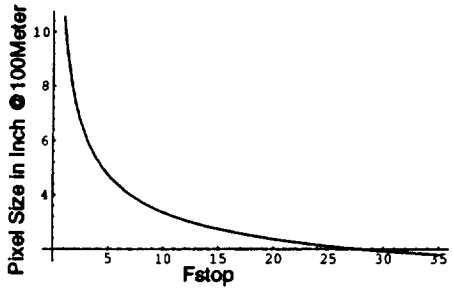

Figure 10: Pixel Size at 100 Meter Range versus Fstop.

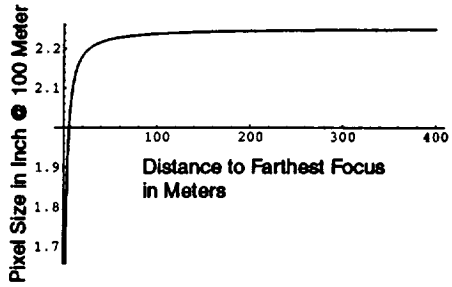

Figure 11: Pixel Size at 100 Meter Range versus Focus Distance for Fstop = 22.

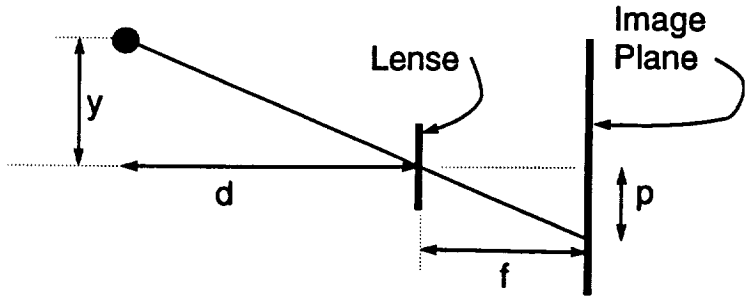

Figure 12: Relation Between Location on Image Plane and Lateral Position (Can Also Be Used to Derive Pixel Size).

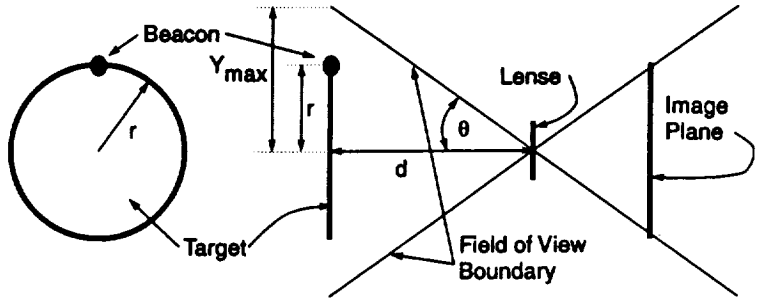

Figure 13: The Maximum Transverse Error Which Can Be Sensed.

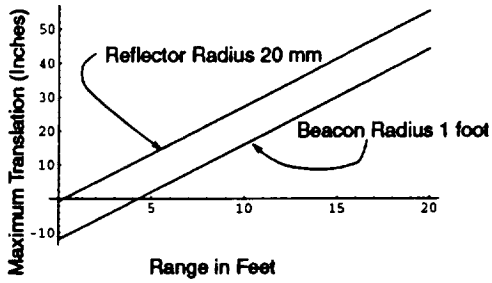

Figure 14: Maximum Translation Before Losing a Beacon.

Performance at Long Ranges

Transverse Position The transverse position of an object can be computed from its image plane location using similar triangles as shown in figure 12 as:

$$y = \frac{pd}{f_i}$$

One concern is the maximum deviation from center which can be tolerated before one or more target beacons/retros leaves the field of view. This distance is shown as Y_{max} in Figure 13. and can be computed as:

$$Y_{max} = d\tan(\theta) - r$$

Figure 14 shows this value versus range. Of particular interest is the point when this becomes zero. At this point, it is impossible to keep all beacons in the field of view. For the specifications (1 foot beacon radius), this occurs at a range of 4.3 inches. For the reflectors (20 mm radius) it is 0.3 inches.

Bearing Angle The pixel size can be used to approximate bearing angle resolution as:

$$\gamma = \tan^{-1}\frac{p}{f_i}$$

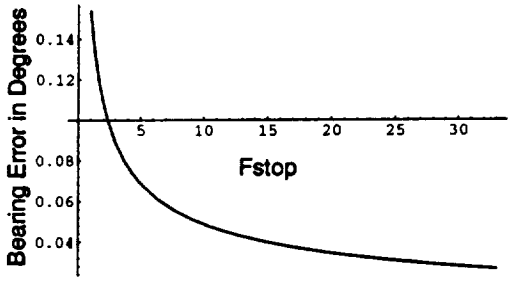

Figure 15: Bearing Error versus Fstop.

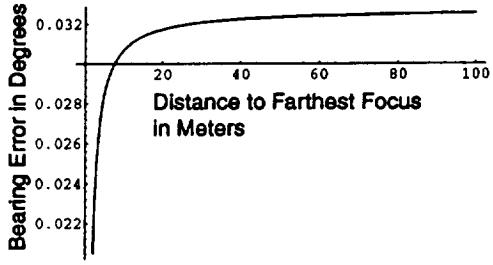

Figure 16: Bearing Error versus Focus Distance for Fstop = 22.

Notice the bearing angle resolution, and hence its rate is constant with respect to the range. For the specifications, the bearing error is 0.0523396°. Figure 15 shows the relation between bearing error and the Fstop. Figure 16 shows the effect of the focus distance on the bearing resolution.

Range Resolution Range is computed by comparing the separation distance between the beacons/reflectors. Using such an algorithm means change in range can only be detected when the separation distance changes. We computed range resolution as the change in range required to produce a distinguishable change in separation. More specifically, we computed the change in range given a change in separation distance (a numerical derivative). Figure 17 For the calculations, we assumed the target is close to centered in the field of view. Based on the specifications, the change in range for a unit change in separation distance is shown in figure 18.

In the software, range was determined using a calibration. The range to perimeter size was empirically determined. The relation between the distance to the target and the perceived perimeter size is an offset hyperbola defined by:

$$d = \frac{a}{D_p} + b$$

At large distances, the perimeter does not change much with distance. At small ranges, the change in perimeter is tremendous. If fact, before the camera lens touches

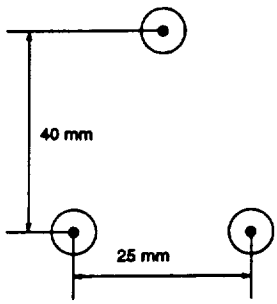

Figure 17: The Retroreflector Target Used.

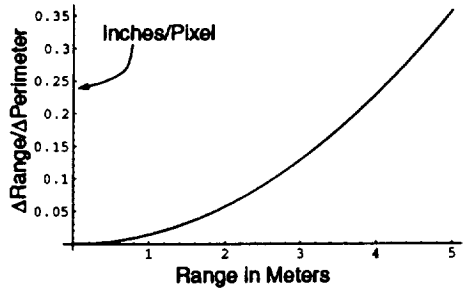

Figure 18: Range Error versus Range.

the mirror ($d = 0$), the entire pattern will no longer be in the camera's view. This relation quickly brings to mind an inverse relationship between the variables. The offset b is necessary because the range is measured from a distance in front of the lens rather than in the middle as theoretically defined. The data shown in Table 2 shows experimental values for range and perimeter. This data was fit to an offset hyperbola where, $a = 149348.9$ mm - pixel and $b = -14.55$ mm. Figure 19 shows the calculated values (as a line) along with the measurements (as symbols).

Attitude Resolution Attitude is determined using an inverse projection transformation. We computed the yaw and pitch attitude error as the smallest change in

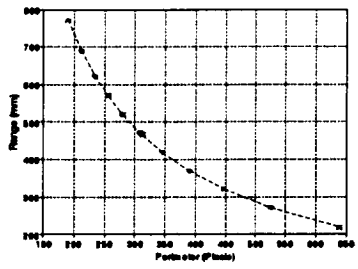

Figure 19: Experimental Range Versus Perimeter.

Perimeter pixels	Range mm
190	769.5
212	688
234	620
256	570
280	520
308	472.5
312	468
345	419.3
390	369.5
447	320
526	268.5
639	218

Table 2: Experimental Range and Perimeter Sizes for the Camera and Target Used At A&M.

attitude that caused the separation distance between two beacons/reflectors (at the same range) to appear to change. Figure 20 shows the smallest yaw and/or pitch required to produce a visible change in the image.

The roll was determined by determining the minimum angle which causes a reflector to move from one pixel to another. The calculation equates the arc length swept by a reflector during a roll to the pixel size. The roll resolution is shown in Figure 21.

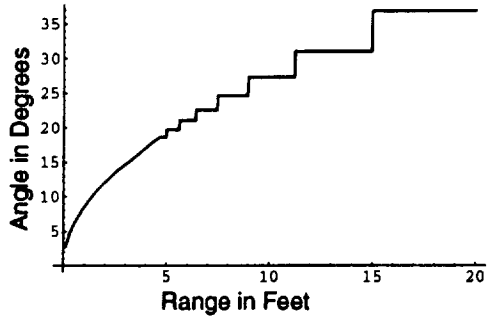

Figure 20: Smallest Recognizable Yaw (or Pitch) Angle Producing Noticeable Change in Image (NonTRAC).

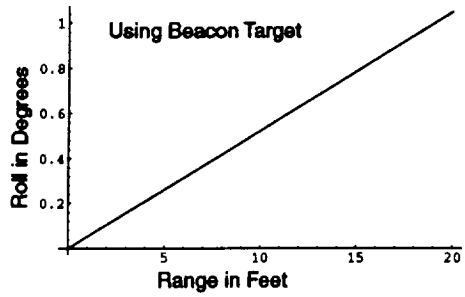

Figure 21: Smallest Recognizable Roll Angle Using Beacons as a Target.

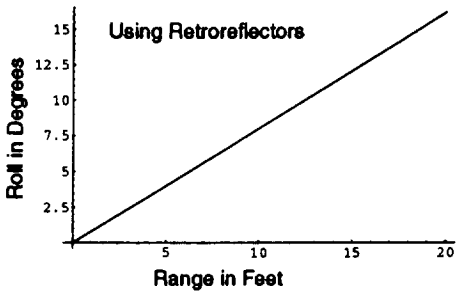

Figure 22: Smallest Recognizable Roll Angle Using Retroreflectors.

Performance at Short Ranges

When in close, the sensing algorithm switches from beacon following into a TRAC system. Determining the transverse position, bearing, range and roll from the TRAC system is identical to that used for long ranges except the beacons are replaced with retroreflections. Numerical differences in the roll resolutions occur because the reflectors have a different configuration (in this study) than the beacons. Based on our specifications, Figure 22 shows the values for the trac system. Since the range calculation depends on the change in perimeter, not in the size of the perimeter, the range resolution is the same for beacons as it is for the reflectors. However, the calibration for the range to pixel conversion is a function of the target.

Attitude Resolution for TRAC Figure 4 demonstrates how TRAC determines the yaw and pitch of the target. It is clear from the diagram that it is equivalent to the calculation of a bearing angle, hence the resolution is independent of the range. For the specifications, the smallest angle measurable by TRAC is 0.0523431 degrees. The maximum angle measurable by TRAC depends predominately on the size of the mirror. Essentially, the reflected image "runs out" the mirror until it falls off the edge. The maximum measurable angle is shown in Figure 23.

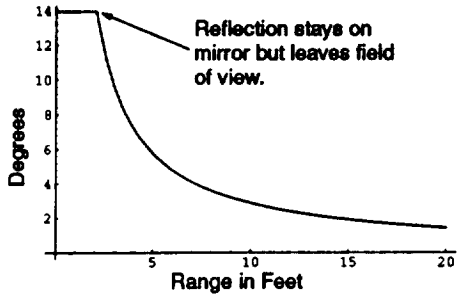

Figure 23: The Maximum Yaw and/or Pitch Angle Measurable by our TRAC.

EXPERIMENTAL EVALUATION

To determine the pitch and yaw resolution, a rotary positioning stage with an accuracy of 0.01° was used to aim the camera at the mirror. The experiment was started with the camera close to normal to the mirror. The camera is then rotated in increments of 0.01° and the pixel changes were recorded. A plot of this data should have a "stair-step" character as the LED in the picture moves between pixels. The experiments were conducted at 2 through 20 feet range.

To measure the horizontal, vertical, and range resolution, the mirror is mounted on a coordinate measuring machine (CMM) that has a resolution of approximately 0.01 mm. This time the CMM moved the mirror and recorded its position while the pixel locations were recorded. Since the range measurement is based on the perimeter of the three retro-reflectors, the resolution of this measurement is dependent on the retro-reflector configuration. This test used an isosceles triangle with an actual perimeter of 109 mm. With this system, 5 feet was the maximum range that reliable results were attained do to the amount of illumination available.

Several images were taken at each point and, averaged together. Occasionally, the system would take a bad image but these were discarded.

Experimental Results

The figures which follow show the results. The results indicate that, as predicted in the analysis, angular resolution does not change with range. Figures 24 and 25 show that sub-pixel resolution is possible. The system used for these experiments had a resolution of 1/3 of a pixel. Because the position of all three retro-reflectors were averaged to determine the lateral movements, it is understandable that the accuracy should be 1/3 pixel. The figures also show that the position of the retro-reflectors tended to shift at about the same time so that the plot has a poorly defined stair step character.

Figures 24 and 25 show that the lateral resolution at 2 feet was about 0.5 mm/pixel. Which compares to 0.556869 mm/pixel as predicted via the theory. The lateral resolution (Figures 26 and 27) for the system at 5 feet was about 1.2 mm/pixel (compare this to 1.39217 mm/pixel as predicted via theory).

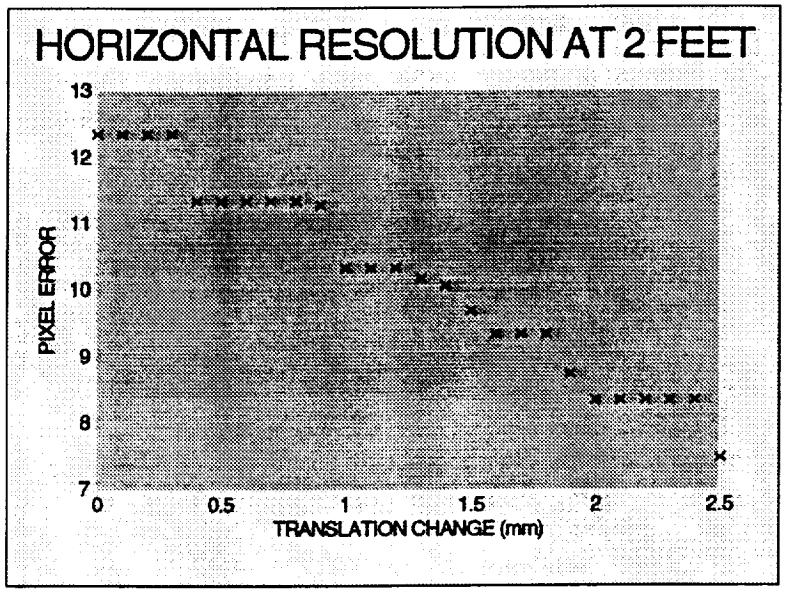

Figure 24:

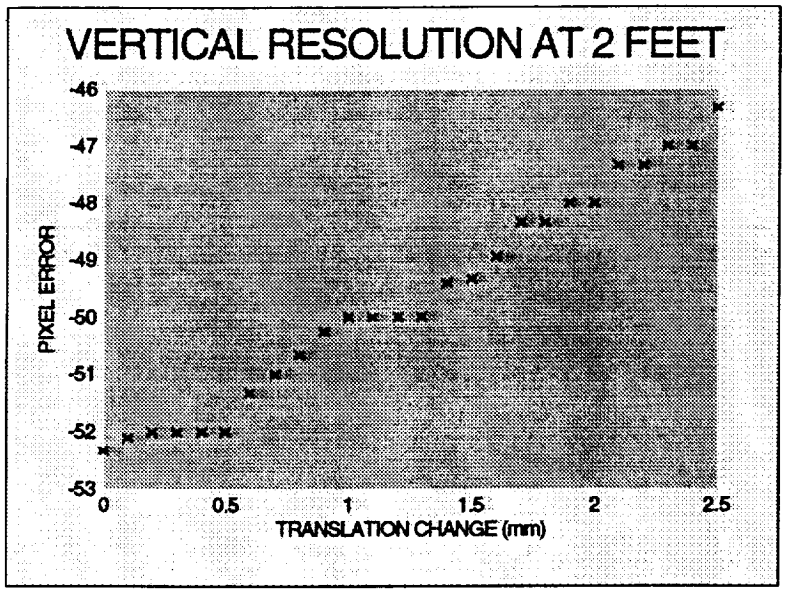

Figure 25:

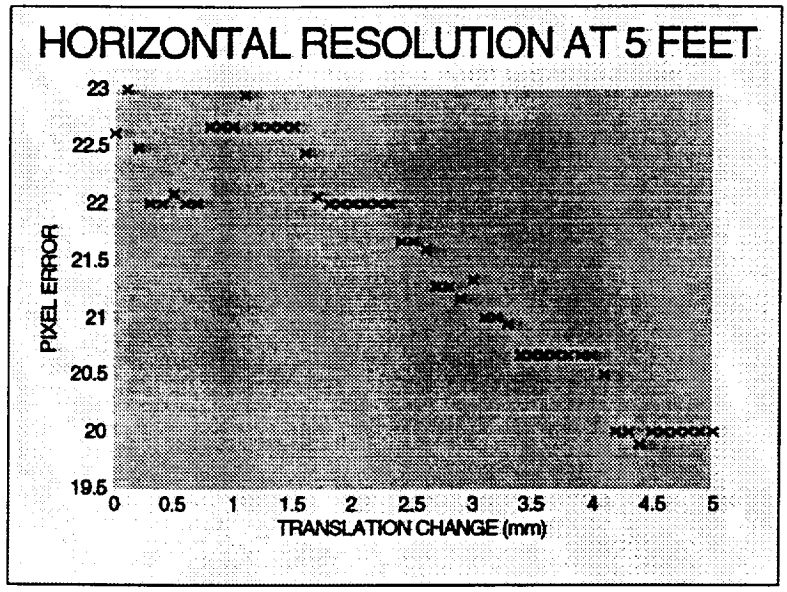

Figure 26:

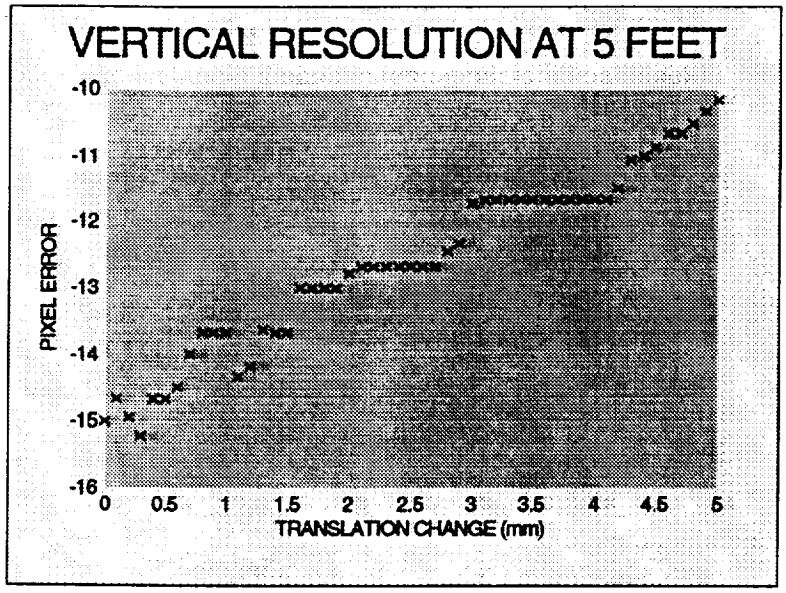

Figure 27:

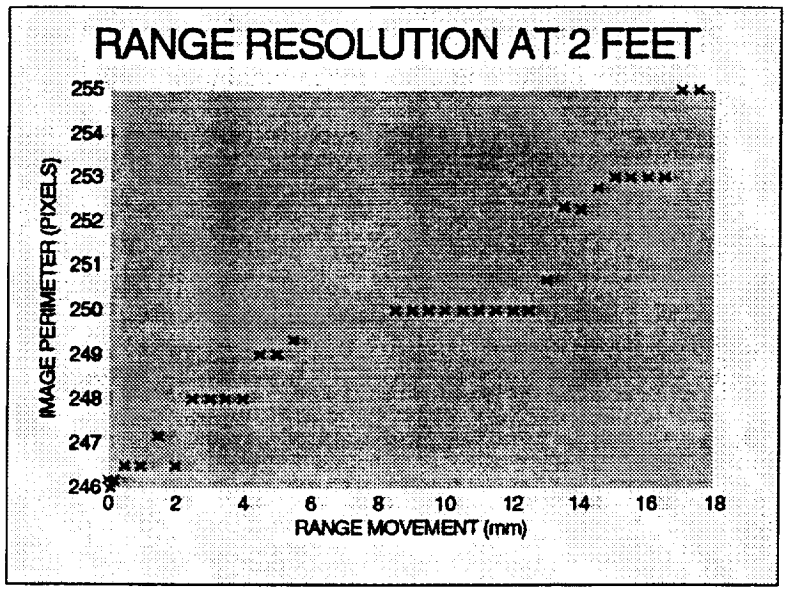

Figure 28:

The range measurement can have sub-pixel resolution because it uses the three retro-reflectors to measure an apparent perimeter of the triangle. Figure 28 shows that the resolution at 2 feet was about 1.8 mm/pixel (compared to 0.197877 by theory). The range resolution at 5 feet was about 19 mm/pixel (compared to 1.23304 by theory). The range resolution is very sensitive to the range. The perimeter is approximately 250 pixels in Figure 28 and about 80 pixels in Figure 29.

The pitch and yaw resolution will not have sub-pixel resolution because it measures the location of the LED reflection only. The angle resolution, determined by Figures 30 and 31, was about 0.045 degrees at 2 feet (compared to 0.0523431 degrees by theory). The transitions were more defined at 2 feet than at the greater distances. The pitch and yaw resolution at 5 feet is determined from Figures 32 and 33. Figures 34 through 35 are angle measurements at 10 through 20 feet. The resolution for these movements, as well as the angle movements for the closer ranges are all about the same (theory predicted them to be independent of range).

The roll resolution at 2 feet was determined differently since actual angle changes are calculated by TRAC rather than pixel changes. Consequently, the experimental points in Figure 36 should fall on a line with slope 1. To measure the resolution, the calculated angle change for each measured (input by the rotation stage) angle change was averaged over the 3° total movement. The vision system averaged about a 0.08° resolution. It is hard to find a good number for the roll resolution at this range because the resolution is of the same order of magnitude as the repeatability of the rotational stage. Figure 37 shows that this isn't true at a range of 5 feet. The resolution at 5 feet is about 1.56° (compared to 1.99454° from theory[3]) which shows

[3]For this calculation, the reflector radius was taken to be 40 mm which compares closer to the

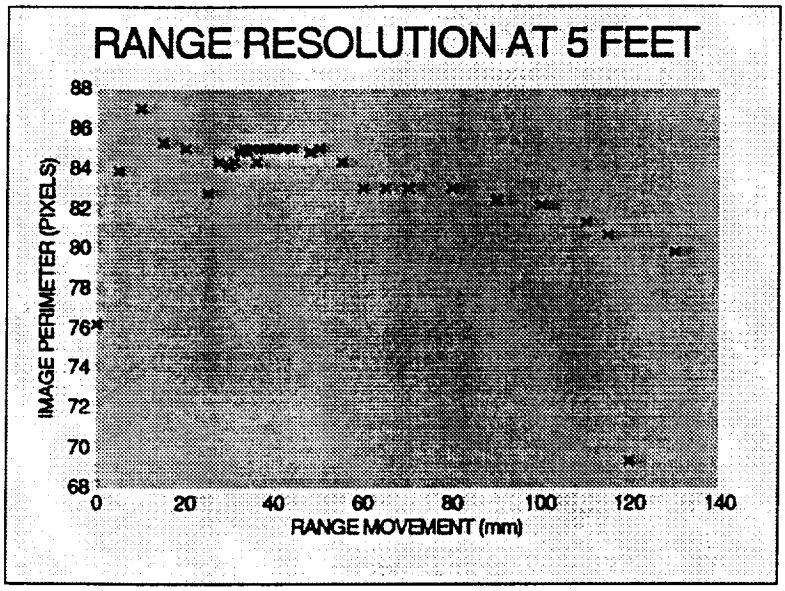

Figure 29:

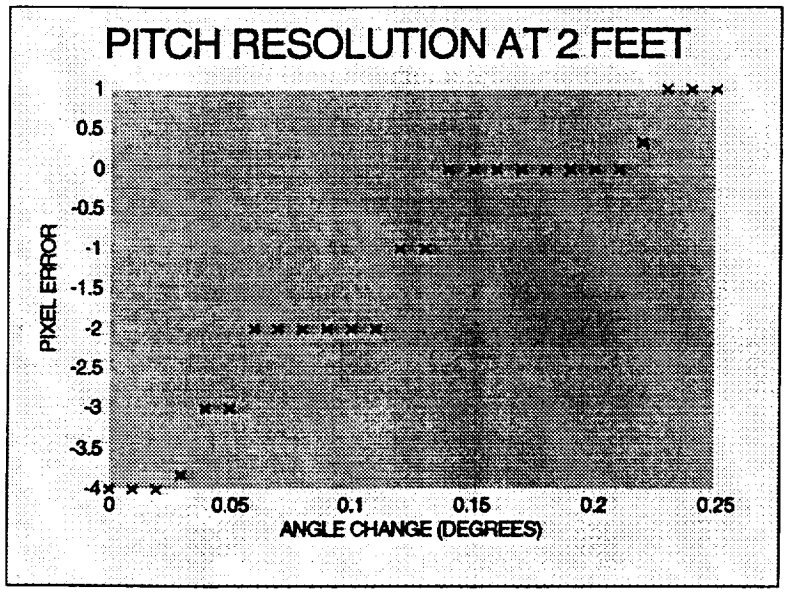

Figure 30:

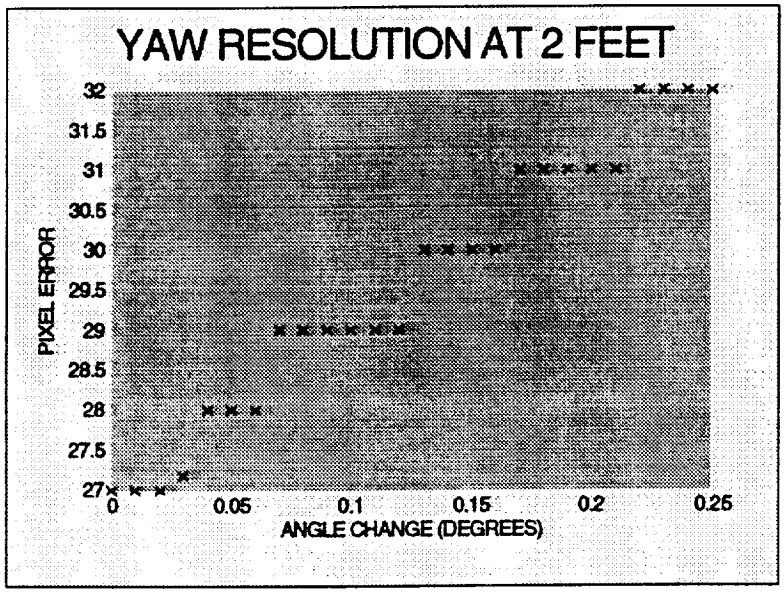

Figure 31:

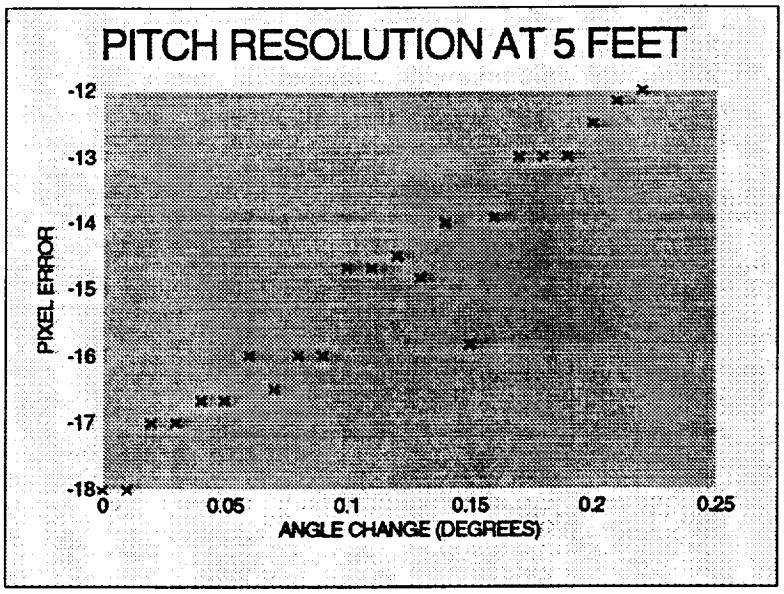

Figure 32:

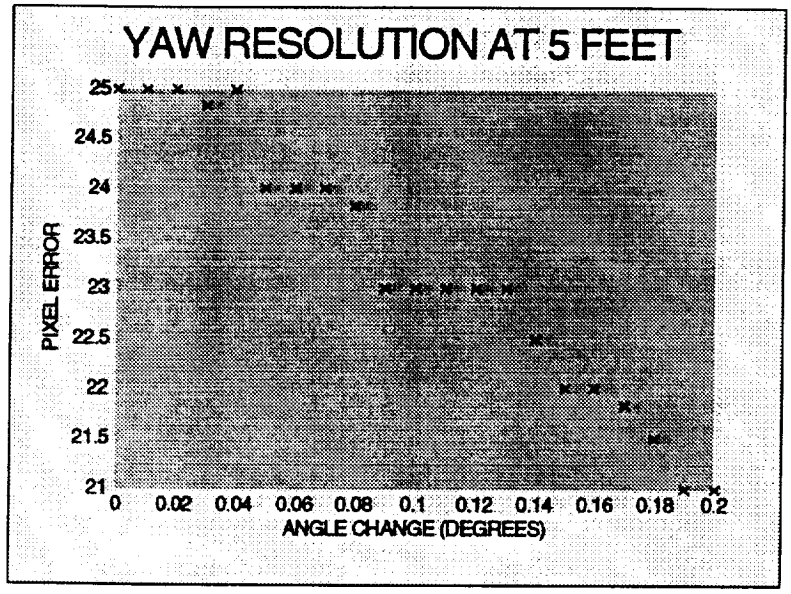

Figure 33:

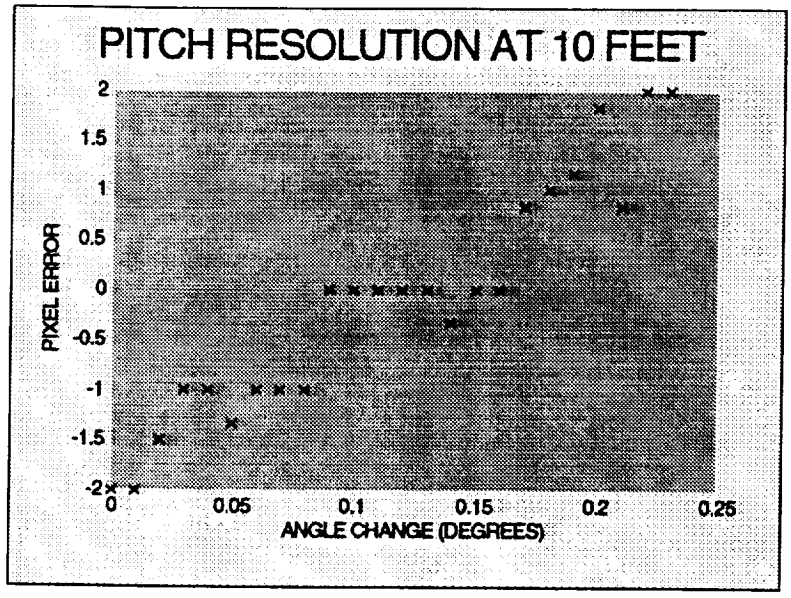

Figure 34:

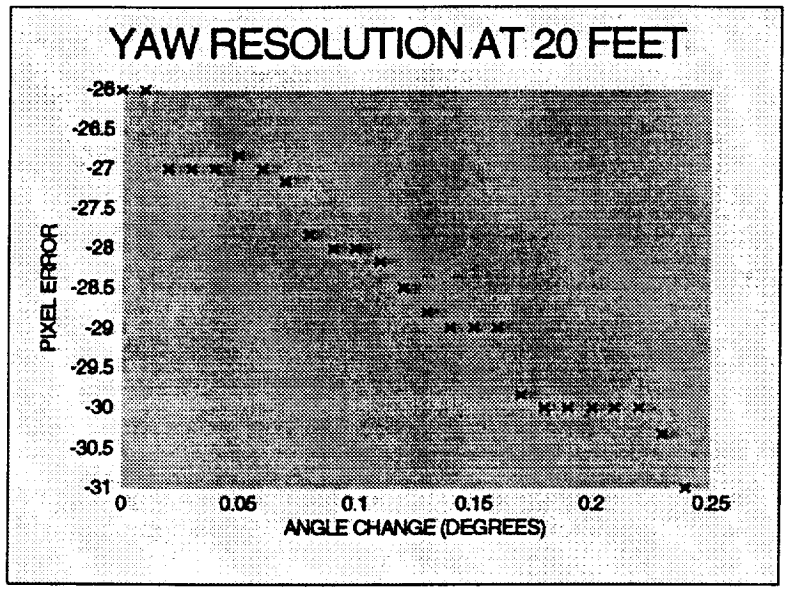

Figure 35:

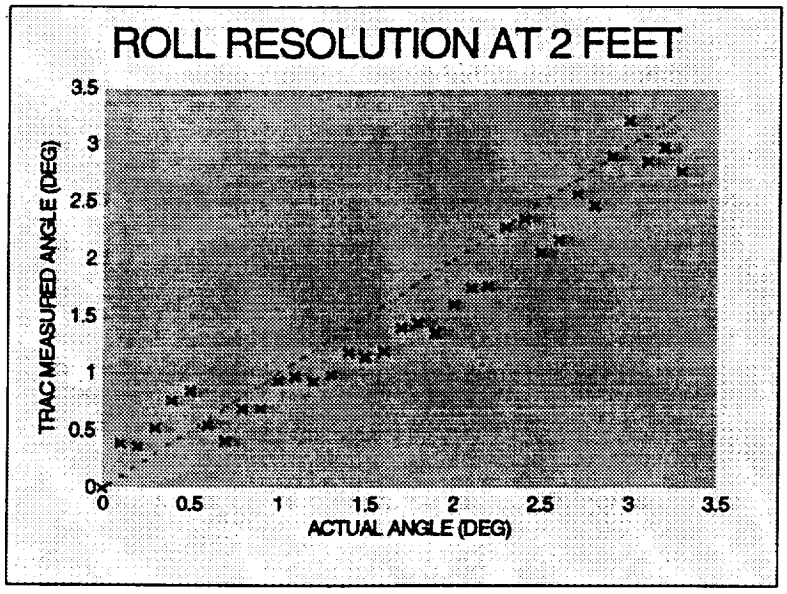

Figure 36:

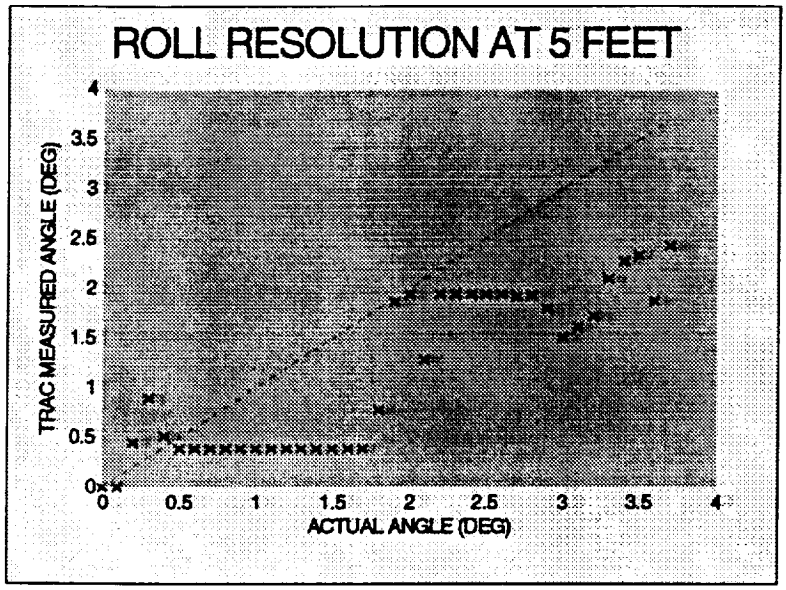

Figure 37:

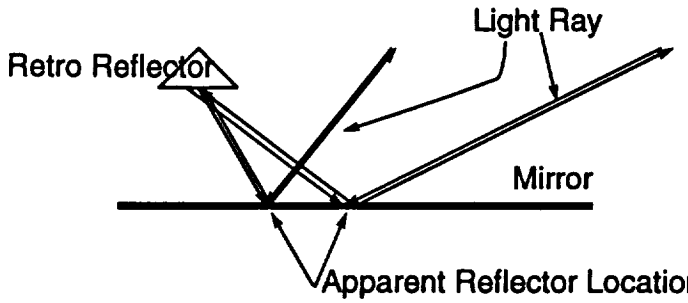

Figure 38: A Proposed Method for Improving the Field of View of a TRAC Sensor.

that roll measurement is very dependent on range as we predicted.

CONCLUSIONS

The chief limitation of the the TRAC sensor is its restricted "field of view". When using the TRAC based sensor, the maximum yaw and pitch deviation is set by the physical size of the target mirror. Essentially the reflection "walks" out the mirror until it falls off. The field of view may be relaxed by using a slightly curved mirror, but this is significantly reduces the illumination returned by the target. Figure 38 When the orientation of the mirror changes, the incident light rays strike at different angles. This causes the apparent location of the reflector to change and hence can be related to orientation.

value used in the software algorithm.

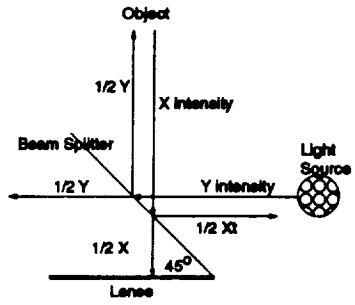

Figure 39: A Beam Splitter Used in Illumination.

Another weakness is when the sensor is used without the TRAC mirror. In this mode, the orientation resolutions are bad. This situation can be improved significantly by elevating one of the reflectors/beacons out of plane.

Another system problem is distinguishing the LED image from the retros. An easy method to handle this problem is to locate the retros on the outside of the mirror. This way, the LED image will always appear inside the retros. The problem of course is that either the TRAC mirror is small or one runs the risk of "losing sight" of the retros at close range.

Another difficulty is obtaining sufficient illumination. The retros do not return much of the light (due to their spreading effects and their size). Perhaps using very bright illumination sources (even strobes in the worst case) implemented either directly mounted on the lense, or at the side of a lense through a beam splitter as shown in figure 39.

One of the significant benefits of the TRAC system is that it has an excellent pitch and yaw resolution. In addition, this resolution is independent of range. In the proper application, these two advantages can prove to be very important.

REFERENCES

[1] L. Monford, "Docking alignment system," U. S. Patent No. 4890918, NASA JSC Case No. MSC 21372-1.

[2] R. Redfield, L. J. Everett, M. Bradham, and J. Pafford, "Autonomous TRAC," Final Report for NASA Grant NAG3-96, Texas A&M University, Mechanical Engineering Department, College Station, TX 77843-3123, December 1991.

[3] *Solid-State Imaging Devices, Tech Note No. T1007.* Vicon Industries Inc., 525 Broad Hollow Road, Melville, Ny 11747-3703, August 1988.